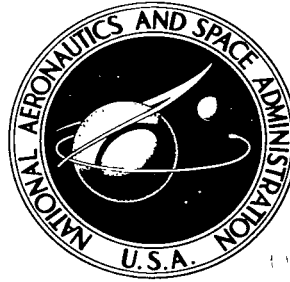


NASA TECHNICAL NOTE



NASA TN D-2784

NASA TN D-2784



0079657

TECH LIBRARY KAFB, NM

THERMAL, FIELD EMISSION WITH A TERMINATED IMAGE POTENTIAL

by James F. Morris

*Lewis Research Center
Cleveland, Ohio*



THERMAL, FIELD EMISSION WITH A TERMINATED IMAGE POTENTIAL

By James F. Morris

Lewis Research Center
Cleveland, Ohio

NATIONAL AERONAUTICS AND SPACE ADMINISTRATION

For sale by the Clearinghouse for Federal Scientific and Technical Information
Springfield, Virginia 22151 - Price \$1.00

THERMAL, FIELD EMISSION WITH A TERMINATED IMAGE POTENTIAL

by James F. Morris

Lewis Research Center

SUMMARY

This paper develops a theory for thermal, field emission with an image potential that terminates at the emitter Fermi level. The resulting equations predict currents over and through the confining potential barrier. In addition, penetration probabilities and their generating functions are tabulated for fields from 10^5 to 10^9 volts per centimeter and for all emitter Fermi levels and work functions. Results are compared with those obtained for the nonterminated image potential.

INTRODUCTION

Interest in the effects of high electric fields on electron emission increases steadily. This growing importance of thermal, field emission is the result of better products. Many electronic devices improve, and new ones evolve with the accelerating utilization of dense currents from intense fields. Furthermore, the use of thermal, field emission in instrumentation and microscopy expands continuously. Therefore, there is a need to understand better the mechanism of electron emission, and this theoretic work aims at that goal.

Electron emission increases in two ways when the electric field applied to the emitter rises. The field reduces both the height and the width of the potential barrier that confines the electrons; thus, more current passes over and through the diminished barrier. Both suprabarrier and intrabarrier emission processes are examined in the present study.

The electron escape rate at high fields depends strongly on the value at which the freespace potential ends on the emitter face. For this reason, most theoretic approaches to thermal, field emission began with some type of terminated image potential, but for simplicity, the ordinary (nonterminated) image potential was used in the derivations. In this work, an image potential that joins the surface at the Fermi level is used throughout. Because a surface potential higher than the Fermi level is difficult to justify, thermal, field emission theories for the nonterminated image potential (NIP) and this terminated version (TIP) probably bracket reality.

The present paper presents approximations for suprabarrier emission (Richardson-Dushman, Schottky, and zero- and first-order TIP). IntrabARRIER emission is indicated by a tabulation of penetration probabilities for fields from 10^5 to 10^9 volts per centimeter and for all emitter Fermi levels and work functions. With these transmission coefficients, the electron supply function, and the suprabarrier emission equation, the total thermal, field emission current can be estimated.

THEORY

The object of this quest is the prediction of suprabarrier and intrabARRIER thermal-field emission for an image potential that terminates at the Fermi level on the emitter face.

TIP Barrier

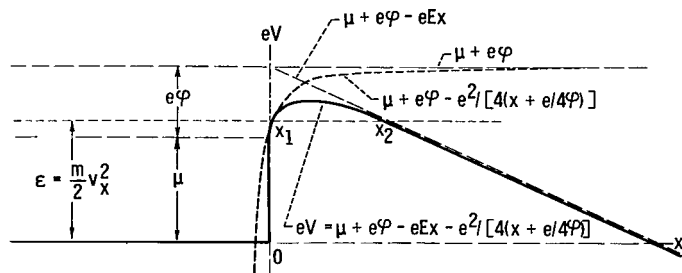
Traditionally, the simple image potential connects with some arbitrary curvature to the bottom of the conduction band at the surface of the emitter (ref. 1). This alters the potential barrier slightly from that for the nonterminated image except at high field intensities. Therefore, the complications of the terminated image potential yielded to the simplicity of the ordinary image in most developments. At moderate fields, this is an appropriate approximation, but what are the high-field effects of a TIP?

In picking the point of potential termination, superficial conditions must be considered. Because surface atoms cannot satisfy their electron needs by lattice continuation, they attract electrons and unbalance the local charge. Furthermore, space-charge equilibrated emission hangs a compact cloud of electrons about emitter boundaries; thus, the electron potential rises sharply at the face of the metal.

A near-equilibrium condition must prevail for any simple emission theory to apply. In this model, the Fermi level remains constant throughout the metal, and the great number of electrons near the Fermi level satisfies the need for excess surface electrons with negligible depletion of the bulk distribution. Therefore, it appears that the electron potential might approach but not exceed the Fermi level at the surface of a pure metal.

For this reason, an image potential that ends at the Fermi level on the emitter face was chosen as the other limit of a range of simple theories for thermal, field emission that begins with the ordinary image.

Because the path between the superficial and internal emitter electron potentials is unknown, the present model sides with simplicity and drops from the Fermi level to



the bottom of the conduction band on the surface. This vertical wall and its crowning corner create questions of electron reflections at abrupt potential changes. The wall and corners of the TIP model, however, are mere approximations of a rapidly but smoothly changing potential; they have no physical significance. Further-

Figure 1 diagrams the barrier formed when the potentials for a freespace electron and for the metal connect at the emitter surface (Symbols are defined in the appendix). Propst (ref. 2) used this type of TIP to predict the energy distribution of electrons ejected from tungsten by low-energy helium ions (He^+).

TIP Suprabarrier Emission

$$eV = \mu + e\varphi - eEx - \frac{e^2}{4\left(x + \frac{e}{4\varphi}\right)} \quad (1)$$

$$x_{\max} = \frac{e}{2(eE)^{1/2}} - \frac{e}{4\varphi} \quad (2)$$

$$eV_{\max} = \mu + e\varphi - (e^3 E)^{1/2} + \frac{e^2 E}{4\varphi} \quad (3)$$

for fields up to $\phi^2 \times 10^8 / 3.6$ volts per centimeter; higher fields maintain the maximum potential at the Fermi level on the emitter surface.

Of course, in the NIP case,

$$x_{\max} = \frac{e}{2(eE)^{1/2}}$$

and

$$eV_{\max} = \mu + e\phi - (e^3 E)^{1/2}$$

The potential maximum equals the minimum kinetic energy (based on the outwardly directed velocity component) that an internal electron requires to escape the emitter in simple suprabarrier emission theory.

These outgoing electrons within the metal distribute in the following manner (ref. 3):

$$\begin{aligned} n(v_x)dv_x &= m dv_x \int_{-\infty}^{\infty} \int_{-\infty}^{\infty} n(p)dp_y dp_z \\ &= \frac{4\pi m^2 kT}{h^3} dv_x \int_0^{\infty} \frac{e^{-\left\{\left[\left(p_{yz}^2 + p_x^2\right)/2m\right] - \mu\right\}/kT} p_{yz} dp_{yz}}{1 + e^{-\left\{\left[\left(p_{yz}^2 + p_x^2\right)/2m\right] - \mu\right\}/kT}} \\ &= \frac{4\pi m^2 kT}{h^3} \ln \left\{ 1 + e^{\left[\mu - (m/2)v_x^2\right]/kT} \right\} dv_x \quad (4) \end{aligned}$$

This distribution, integrated from the potential barrier maximum to infinity, yields the equation for suprabarrier emission:

$$\begin{aligned}
j_{\text{TIP}} &= \frac{4\pi m^2 \kappa T e}{h^3} \int_{(2eV_{\text{max}}/m)^{1/2}}^{\infty} \ln \left\{ 1 + e^{-\left[(m/2)v_x^2 - \mu\right]/\kappa T} \right\} \frac{\kappa T}{m} \frac{mv_x dv_x}{\kappa T} \\
&= \frac{4\pi m(\kappa T)^2 e}{h^3} \int_{\infty}^{eV_{\text{max}}} \ln \left[1 + e^{-\left(\epsilon - \mu\right)/\kappa T} \right] \left(-\frac{d\epsilon}{\kappa T} \right) \\
&= \frac{4\pi m(\kappa T)^2 e}{h^3} \left\{ e^{-\left[e\phi - (e^3 E)^{1/2} + (e^2 E/4\phi)\right]/\kappa T} - \frac{e^{-2\left[e\phi - (e^3 E)^{1/2} + (e^2 E/4\phi)\right]/\kappa T}}{4} \right. \\
&\quad \left. + \frac{e^{-3\left[e\phi - (e^3 E)^{1/2} + (e^2 E/4\phi)\right]/\kappa T}}{9} - \frac{e^{-4\left[e\phi - (e^3 E)^{1/2} + (e^2 E/4\phi)\right]/\kappa T}}{16} + \dots \right\} \quad (5)
\end{aligned}$$

The zero-order approximation is the TIP version of the Schottky equation.

Approximation for Suprabarrier Emission

Two suprabarrier emission equations compare clearly as the log of the ratio of their current densities for a given set of conditions. This approach eliminates debates about effective areas and coefficients ($120T^2$) and reduces the comparison to the difference of two exponents. An electric-field effect might then be considered significant when the current-density ratio for the two emission equations reaches 1.001 or 0.999. This is the comparative criterion in the following evaluations for T in $^{\circ}\text{K}$, ϕ in volts, and E in volts per centimeter.

With these stipulations, little effort is required to isolate the areas of apparent applicability of Richardson-Dushman (RD), Schottky (S), and zero- (TIP-0) and first-order (TIP-I) TIP approximations for suprabarrier electron emission.

In the following comparisons, the particular emission equation appears immediately after its name and is attended by the electric field at which its current density

differs by 0.1 percent from that of the next more complicated emission expression; of course, if the field were increased, the difference would be greater:

Richardson-Dushman:

$$j_{RD} = 120T^2 \exp\left(-\frac{e\varphi}{\kappa T}\right)$$

$$\frac{j_{RD}}{j_S} = 0.999 \quad \text{at } E = 5.16T^2 \times 10^{-8}$$

Schottky (NIP):

$$j_S = 120T^2 \exp\left[-\frac{e\varphi - (e^3 E)^{1/2}}{\kappa T}\right]$$

$$\frac{j_S}{j_{TIP-0}} = 1.001 \quad \text{at } E = 2.4 \varphi T$$

Zero-order TIP:

$$j_{TIP-0} = 120T^2 \exp\left[-\frac{e\varphi - (e^3 E)^{1/2} + \frac{e^2 E}{4\varphi}}{\kappa T}\right]$$

$$\frac{j_{TIP-0}}{j_{TIP-I}} = 1.001 \quad \text{at } E = 0.278\varphi^2 \left[1 + 2.18\left(\frac{T}{\varphi}\right)^{1/2} \times 10^{-2}\right]^2 \times 10^8$$

First-order TIP:

$$j_{TIP-I} = 120T^2 \left\{ e^{-\left[\frac{e\varphi - (e^3 E)^{1/2} + (e^2 E/4\varphi)}{\kappa T}\right]} - \frac{e^{-2\left[\frac{e\varphi - (e^3 E)^{1/2} + (e^2 E/4\varphi)}{\kappa T}\right]}}{4} \right\}$$

Both the TIP and NIP equations raise questions when fields rise to near 10^7 volts per centimeter. At this value, the potential maxima for these two models lie between

5 and 6 angstroms from the emitter surface. Because this is near the atomic dimension, the assumptions of the TIP and NIP models approximate the actual physical situation poorly.

TIP Tunneling

The kinetic energy of a tunneling electron is negative, and therefore, its momentum is imaginary. So within the emission barrier, an electron lies less likely at $x + \Delta x$ than at x in accordance with the probability-density ratio for the two locations:

$$P = \frac{\psi^*(x + \Delta x)\psi(x + \Delta x)}{\psi^*(x)\psi(x)} \approx \frac{\exp[-2|k|(x + \Delta x)]}{\exp(-2|k|x)} = \exp(-2|k|\Delta x) \\ = \exp\left\{-\frac{2}{\hbar}\left[2m(eV - \epsilon)\right]^{1/2}\Delta x\right\} \quad (6)$$

The product of such successive probability ratios through a barrier for a particular electron indicates the odds for escape by tunneling. This product of incremental probability ratios merely requires a summation of the exponents; thus, in the limit

$$P \approx \exp\left\{\frac{2}{\hbar} \int_{x_1}^{x_2} \left[2m(eV - \epsilon)\right]^{1/2} dx\right\} \\ = \exp\left\{-\frac{2}{\hbar} \int_{x_1}^{x_2} \left[2m\left(\mu + e\varphi - eEx - \frac{e^2}{4x + \frac{e}{\varphi}} - \epsilon\right)\right]^{1/2} dx\right\} \quad (7)$$

which is an approximation of the WKB result (ref. 1),

$$P = f(\epsilon, V) \exp\left\{-\frac{2}{\hbar} \int_{x_1}^{x_2} \left[2m(eV - \epsilon)\right]^{1/2} dx\right\} \approx \exp\left\{-\frac{2}{\hbar} \int_{x_1}^{x_2} \left[2m(eV - \epsilon)\right]^{1/2} dx\right\} \quad (8)$$

where x_1 and x_2 are the turning points ($\epsilon = eV$) for the barrier (fig. 1).

Consequently, the penetration theory for the TIP emission barrier begins with the assumptions and restrictions of the WKB theory, and that leaves little but the actual integration and evaluation of the transmission coefficient (eq. (7)):

$$\begin{aligned}
P &\approx \exp \left[- \left(\frac{2^3 m}{\hbar^2} \right)^{1/2} \int_{x_1}^{x_2} \left(\mu + e\phi - eEx - \frac{e^2}{4x + e/\phi} - \epsilon \right)^{1/2} dx \right] \\
&= \exp \left\{ - \frac{(2\beta)^{3/2} m^{1/2}}{\hbar e E} \int_{x_1}^{x_2} \left[1 + \frac{e^3 E \beta}{4\beta^2 e\phi} - \frac{eE}{\beta} \left(x + \frac{e}{4\phi} \right) - \frac{e^3 E}{4\beta^2 \frac{eE}{\beta} \left(x + \frac{e}{4\phi} \right)} \right]^{1/2} \frac{eE dx}{\beta} \right\} \\
&= \exp \left\{ - \left(\frac{\alpha}{2} \right)^{-3/2} \left(\frac{\xi}{eE} \right)^{1/4} \int_{\eta_1}^{\eta_2} \left[1 + \left(\frac{\alpha}{2} \right)^2 \delta - \eta - \frac{(\alpha/2)^2}{\eta} \right]^{1/2} d\eta \right\} \quad (9)
\end{aligned}$$

At the turning points,

$$\frac{eV - \epsilon}{\beta} = 0 = 1 + \left(\frac{\alpha}{2} \right)^2 \delta - \eta - \frac{(\alpha/2)^2}{\eta} \quad (10)$$

Therefore,

$$\eta_{2,1} = \frac{1 + (\alpha/2)^2 \delta}{2} \left(1 \pm \left\{ 1 - \frac{4(\alpha/2)^2}{[1 + (\alpha/2)^2 \delta]^2} \right\}^{1/2} \right) \quad \text{for } \delta < 1 \quad (11)$$

When $\delta \geq 1$, however, the inner turning point is not η_1 ; instead, it is $(\alpha/2)^2 \delta$ because $x_1 = 0$. Therefore, at this juncture a generalized inner turning point is defined as η_0 , which is η_1 for $\delta < 1$ and $(\alpha/2)^2 \delta$ for $\delta \geq 1$.

Now, as $\alpha \rightarrow 0$,

$$\int_{\eta_1}^{\eta_2} \left[1 + \left(\frac{\alpha}{2} \right)^2 \delta - \eta - \frac{(\alpha/2)^2}{\eta} \right]^{1/2} d\eta \rightarrow \frac{2}{3} \quad (12)$$

Then, by definition,

$$I(\alpha, \delta) \equiv \frac{3}{2} \int_{\eta_1}^{\eta_2} \left[1 + \left(\frac{\alpha}{2} \right)^2 \delta - \eta - \frac{(\alpha/2)^2}{\eta} \right]^{1/2} d\eta \quad (13)$$

and

$$C(\alpha, E) \equiv \frac{2}{3} \left(\frac{\alpha}{2} \right)^{-3/2} \left(\frac{\xi}{eE} \right)^{1/4} \quad (14)$$

and the penetration probability (eq. (9)) becomes

$$P \approx \exp \left[- C(\alpha, E) I(\alpha, \delta) \right] \quad (15)$$

As $\delta \rightarrow 0$ with nonzero β ,

$$I(\alpha, \delta) \rightarrow I(\alpha) = \frac{3}{2} \int_{\eta_1}^{\eta_2} \left[1 - \eta - \frac{(\alpha/2)^2}{\eta} \right]^{1/2} d\eta \quad (16)$$

and

$$\eta_{2,1} \rightarrow \frac{1}{2} \left[1 \pm (1 - \alpha^2)^{1/2} \right] \quad (17)$$

These forms are identical with those for the nonterminated image potential, because as $\delta \rightarrow 0$, $\varphi \rightarrow \infty$ and causes $TIP \rightarrow NIP$.

Both distances and potentials are real in the TIP model; consequently, α , β , δ , and η are all positive. Therefore, the number under the radical in equation (11) for $\eta_{2,1}$ must fall between zero and one.

$$0 \leq \frac{4(\alpha/2)^2}{\left[1 + (\alpha/2)^2 \delta\right]^2} \leq 1 \quad (18)$$

This limits α for δ 's between zero and one to

$$0 \leq \alpha \leq \frac{2\left[1 - (1 - \delta)^{1/2}\right]}{\delta} \quad (19a)$$

and

$$\infty \geq \alpha \geq \frac{2\left[1 + (1 - \delta)^{1/2}\right]}{\delta} \quad (19b)$$

Each range of α yields positive η_1 's and η_2 's; however, the higher range gives negative values of x . Thus, only the lower α range is physically meaningful; the upper limits for α in the TIP model are shown in table I.

For $\delta > 1$,

$$\frac{4(\alpha/2)^2}{\left[1 + (\alpha/2)^2 \delta\right]^2}$$

cannot climb to unity regardless of the α value; thus, inequality (18) is satisfied.

Now equation (13) can be integrated.

$$\begin{aligned}
I(\alpha, \delta) &= \frac{3}{2} \int_{\eta_0}^{\eta_2} \left[1 + \left(\frac{\alpha}{2} \right)^2 \delta - \eta - \frac{(\alpha/2)^2}{\eta} \right]^{1/2} d\eta = 3 \int_{\eta_0^{1/2}}^{\eta_2^{1/2}} [(\eta_2 - \eta)(\eta - \eta_1)]^{1/2} d(\eta^{1/2}) = \frac{3(\eta_2 - \eta_1)^2}{\eta_2^{1/2}} \int_0^{u_1} \operatorname{sn}^2 u \operatorname{cn}^2 u \, du \\
&= \frac{(\eta_2 - \eta_1)^2}{\eta^{1/2} K^4} \left[(2 - K^2)E(u) - 2K^2 u - K^2 \operatorname{sn} u \operatorname{cn} u \operatorname{dn} u \right]_0^{u_1} \\
&= \frac{(\eta_2 - \eta_1)^2}{\eta_2^{1/2} \left(\frac{\eta_2 - \eta_1}{\eta_2} \right)^2} \left[\left(2 - \frac{\eta_2 - \eta_1}{\eta_2} \right) E(u_1) - 2 \left(1 - \frac{\eta_2 - \eta_1}{\eta_2} \right) u_1 - \frac{\eta_2 - \eta_1}{\eta_2} \left(\frac{\eta_2 - \eta_0}{\eta_2 - \eta_1} \right)^{1/2} \left(1 - \frac{\eta_2 - \eta_0}{\eta_2 - \eta_1} \right)^{1/2} \left(1 - \frac{\eta_2 - \eta_1}{\eta_2} \frac{\eta_2 - \eta_0}{\eta_2 - \eta_1} \right)^{1/2} \right] \\
&= \eta_2^{1/2} (\eta_2 + \eta_1) \left[E(u_1) - \frac{2\eta_1}{\eta_2 + \eta_1} u_1 - \frac{(\eta_2 - \eta_0)^{1/2} (\eta_0 - \eta_1)^{1/2} \eta_0^{1/2}}{\eta_2^{1/2} (\eta_2 + \eta_1)} \right] \\
&= \left\{ \left[1 + \left(\frac{\alpha}{2} \right)^2 \delta \right]^3 \frac{1 + \gamma}{2} \right\}^{1/2} \left[E(\Phi, K) - (1 - \gamma) F(\Phi, K) - \left(\frac{\eta_0 \left\{ \left[1 + \left(\frac{\alpha}{2} \right)^2 \delta \right] \eta_0 - \eta_0^2 - \left(\frac{\alpha}{2} \right)^2 \right\}^{1/2}}{\left[1 + \left(\frac{\alpha}{2} \right)^2 \delta \right]^3 \frac{1 + \gamma}{2}} \right)^{1/2} \right] \quad (20)
\end{aligned}$$

where

$$\begin{aligned}
\gamma &= \left\{ 1 - \frac{4(\alpha/2)^2}{\left[1 + (\alpha/2)^2 \delta \right]^2} \right\}^{1/2} \\
K &= \left(\frac{2\gamma}{1 + \gamma} \right)^{1/2}
\end{aligned}$$

and, of course, $F(\Phi, K)$ and $E(\Phi, K)$ are incomplete elliptic integrals of the first and second kinds, respectively.

Because $\eta_0 = \eta_1$ for $\delta < 1$ and $\eta_0 = (\alpha/2)^2 \delta$ for $\delta \geq 1$, two solutions for $I(\alpha, \delta)$ result. For $\delta < 1$,

$$\Phi = \sin^{-1} \left(\frac{\eta_2 - \eta_0}{\eta_2 - \eta_1} \right)^{1/2} = \frac{\pi}{2} \quad (21)$$

and

$$I(\alpha, \delta) = \left\{ \left[1 + \left(\frac{\alpha}{2} \right)^2 \delta \right]^3 \left(\frac{1+\gamma}{2} \right) \right\}^{1/2} \left\{ E \left[\left(\frac{2\gamma}{1+\gamma} \right)^{1/2} \right] - (1-\gamma) F \left[\left(\frac{2\gamma}{1+\gamma} \right)^{1/2} \right] \right\} \quad (22)$$

where $F(K)$ and $E(K)$ are complete elliptic integrals of the first and second kinds, respectively. For $\delta \geq 1$,

$$\Phi = \sin^{-1} \left(\frac{\eta_2 - \eta_0}{\eta_2 - \eta_1} \right)^{1/2} = \sin^{-1} \left\{ \frac{\frac{1+\gamma}{2} - \left(\frac{\alpha}{2} \right)^2 \delta / \left[1 + \left(\frac{\alpha}{2} \right)^2 \delta \right]}{\gamma} \right\}^{1/2} \quad (23)$$

and

$$\begin{aligned} I(\alpha, \delta) = & \left\{ \left[1 + \left(\frac{\alpha}{2} \right)^2 \delta \right]^3 \frac{1+\gamma}{2} \right\}^{1/2} \left[E \left(\sin^{-1} \left\{ \frac{\frac{1+\gamma}{2} - \left(\frac{\alpha}{2} \right)^2 \delta / \left[1 + \left(\frac{\alpha}{2} \right)^2 \delta \right]}{\gamma} \right\}^{1/2}, \left(\frac{2\gamma}{1+\gamma} \right)^{1/2} \right) \right. \right. \\ & - (1-\gamma) F \left(\sin^{-1} \left\{ \frac{\frac{1+\gamma}{2} - \left(\frac{\alpha}{2} \right)^2 \delta / \left[1 + \left(\frac{\alpha}{2} \right)^2 \delta \right]}{\gamma} \right\}^{1/2}, \left(\frac{2\gamma}{1+\gamma} \right)^{1/2} \right) \\ & \left. \left. - \left\{ \frac{\delta \left(\frac{\alpha}{2} \right)^4 (\delta - 1)}{\left[1 + \left(\frac{\alpha}{2} \right)^2 \delta \right]^3 \frac{1+\gamma}{2}} \right\}^{1/2} \right] \right] \quad (24) \end{aligned}$$

Values of $C(\alpha, E)$, $I(\alpha, \delta)$, and P are given in tables II to IV. More P values can be computed with other permutations of the tabulated C and I results.

These penetration probabilities can be used with the distribution function for outgoing electrons (eq. (4)) to predict tunneling currents for the TIP emission barrier.

The ranges of parameters for which C , I , and P are tabulated are extreme; certain of these parametric combinations produce conditions that preclude simple emission-barrier models or that cannot be realized physically. Therefore, the limitations of thermal, field emission theory should be checked before the results are applied.

Limitations of Thermal, Field Emission Theories

First, the effects of the TIP on thermal, field emission can be observed. TIP suprabarrier emission was compared with the Schottky (NIP) equation in an earlier section (Approximations for Suprabarrier Emission). The previous section and tables II to IV examine the NIP and TIP penetration probabilities; values for $\delta = 0$ are identical with NIP transmission coefficients (ref. 4). The differences between NIP and TIP theories are therefore obvious.

Neither the NIP nor the TIP barrier model stands under certain extreme conditions. For example, when the distance from the emitter face to the outside of the barrier reduces to near-atomic dimensions, the assumption of a smooth metal surface fails. Furthermore, if the emission density becomes a significant fraction of the internal electron density, the near-equilibrium assumption fails, and the Fermi-Dirac distribution cannot be used. Since these are high-field symptoms, both the NIP and TIP theories decrease in applicability as the electric field increases.

In addition to these simple problems, penetration difficulties must be considered. It was noted earlier that reflections caused by abrupt potential changes are not considered in the NIP and TIP models. It was also mentioned that the WKB restrictions apply; these requirements reside in the expression

$$\left| \frac{d\lambda}{dx} \right| = \left| \frac{\hbar}{p^2} \frac{dp}{dx} \right| \ll 1 \quad (25)$$

which is the condition for negligible reflection of an electron wave. Obviously, then, the WKB approximation falters when $p \rightarrow 0$; this condition occurs near the turning points and near the maximum of the emission barrier. Electrons, however, that have a finite p as they pass under the barrier maximum adhere to WKB principles exactly, because $dp/dx = 0$ there. But the electron momentum function must satisfy equation (25) throughout much of the integration for $I(\alpha, \delta)$ for a good approximation.

Then there is the function $f(\epsilon, V)$ that multiplies the exponential in the complete WKB penetration probability (eq. (8)). The need for this function is debatable, and in any event, it causes differences of less than a factor of two in transmission coefficients at pertinent energy levels (ref. 5). If this refinement is deemed necessary, however, the present penetration probabilities can be multiplied by some apparently appropriate $f(\epsilon, V)$.

Finally, when all of these conditions have been properly met, the TIP results can be used to approximate thermal, field emission.

Lewis Research Center,

National Aeronautics and Space Administration,

Cleveland, Ohio, January 21, 1965.

APPENDIX - SYMBOLS

$C(\alpha, E)$	coefficient in exponent of penetration probability	P	penetration probability
E	electrostatic field, V/cm	p	electronic momentum
$E(K)$	complete elliptic integral of second kind	T	absolute temperature, $^{\circ}\text{K}$
$E(\Phi, K)$	incomplete elliptic integral of second kind	TIP	$-e^2/(4x + e/\varphi)$, also refers to emission model using image potential that terminates at Fermi level on emitter surface
e	electronic charge	V	potential
$F(K)$	complete elliptic integral of the first kind	v	velocity
$F(\Phi, K)$	incomplete elliptic integral of the first kind	x	dimension normal to emitter surface
f	function	y	dimension in emitter surface
h	Planck's constant	z	dimension normal to x and y
\hbar	Planck's constant divided by 2π	α	$e(eE)^{1/2}/\beta$
$I(\alpha, \delta)$	integral in exponent of penetration probability	β	$\mu + e\varphi - \epsilon$
i	imaginary	γ	$\left\{1 - 4(\alpha/2)^2/[1 + (\alpha/2)^2\delta^2]\right\}^{1/2}$
j	current density, A/sq cm	δ	$\beta/e\varphi$
k	wave number for electron wave	ϵ	$mv_x^2/2$
K	modulus of elliptic integral	η	$eE(x + e/4\varphi)/\beta$
m	electronic mass	κ	Boltzmann constant
NIP	$-e^2/4x$, also refers to emission model using ordinary image potential	λ	wavelength of electron wave
$n(p)$	electron number density in phase space	μ	Fermi level
$n(v_x)$	electron number density dimensional and x -directed velocity space	ξ	$e^6 m^2/\hbar^4$
		Φ	upper limit of elliptic integral
		φ	work function
		Ψ	electronic wave function

ψ^* complex conjugate of ψ

Subscripts:

max maximum potential location

RD Richardson-Dushman

S Schottky

TIP terminated image potential

TIP-0 TIP zero-order approximation

TIP-I TIP first-order approximation

x, y, z x, y, or z dimension

yz y-z dimension space

0 generalized inside turning point on emission barrier

1 inner turning point above Fermi level on emission barrier

2 outer turning point on emission barrier

REFERENCES

1. Bohm, David: Quantum Theory. Prentice-Hall Inc., 1961.
2. Propst, F. M.: Energy Distribution of Electrons Ejected from Tungsten by He^+ . Phys. Rev., vol. 129, no. 1, Jan. 1963, pp. 7-11.
3. Sommerfeld, A.; and Bethe, H.: Elektronentheorie der Metalle. Handbuch der Physik. Springer-Verlag (Berlin), vol. 24, pt. 2, 1933, pp. 333-622.
4. Burgess, R. E.; Kroemer, H.; and Houston, J. M.: Corrected Values of Fowler-Nordheim Field Emission Functions $v(y)$ and $s(y)$. Phys. Rev., vol. 90, no. 4, May 15, 1953, p. 515.
5. Dyke, W. P.; and Dolan, W. W.: Field Emission. Vol. VIII of Advances in Electronics and Electron Physics, L. Marton, ed., Academic Press, 1956, p. 93.

TABLE I. - UPPER LIMITS OF α

FOR TIP MODEL

	δ							
	0	0.1	0.2	0.4	0.6	0.8	0.9	1
α	1	1.03	1.06	1.13	1.23	1.38	1.52	2

TABLE II. - COEFFICIENT IN EXPONENT OF PENETRATION PROBABILITY

α	Electrostatic field, E, V/cm								
	10^5	$10^{5.5}$	10^6	$10^{6.5}$	10^7	$10^{7.5}$	10^8	$10^{8.5}$	10^9
0.0000	∞	∞	∞	∞	∞	∞	∞	∞	∞
.1000	898.05	673.44	505.01	378.71	283.99	212.96	159.70	119.76	89.805
.2000	317.51	238.10	178.55	133.89	100.41	75.293	56.462	42.341	31.751
.4000	112.26	84.180	63.126	47.338	35.499	26.620	19.962	14.970	11.226
.6000	61.105	45.822	34.362	25.768	19.323	14.490	10.866	8.1484	6.1105
.8000	39.689	29.762	22.319	16.737	12.551	9.4117	7.0577	5.2926	3.9689
.9000	33.261	24.942	18.704	14.026	10.518	7.8875	5.9148	4.4354	3.3261
1.0000	28.399	21.296	15.970	11.976	8.9805	6.7344	5.0501	3.7871	2.8399
1.0263	27.313	20.482	15.359	11.518	8.6371	6.4769	4.8570	3.6422	2.7313
1.0557	26.180	19.632	14.722	11.040	8.2789	6.2083	4.6556	3.4912	2.6180
1.1270	23.736	17.799	13.348	10.009	7.5059	5.6287	4.2209	3.1652	2.3736
1.2000	21.604	16.201	12.149	9.1102	6.8317	5.1231	3.8418	2.8809	2.1604
1.2251	20.942	15.704	11.777	8.8312	6.6224	4.9661	3.7241	2.7927	2.0942
1.3820	17.481	13.109	9.8300	7.3715	5.5278	4.1453	3.1085	2.3311	1.7481
1.4000	17.144	12.856	9.6407	7.2295	5.4214	4.0655	3.0487	2.2862	1.7144
1.5195	15.162	11.370	8.5261	6.3937	4.7946	3.5954	2.6962	2.0219	1.5162
2.0000	10.041	7.5293	5.6462	4.2341	3.1751	2.3810	1.7855	1.3389	1.0041
4.0000	3.5499	2.6620	1.9962	1.4970	1.1226	.84180	.63126	.47338	.35499
10.0000	.89805	.67344	.50501	.37871	.28399	.21296	.15970	.11976	.089805
20.0000	.31751	.23810	.17855	.13389	.10041	.075293	.056462	.042341	.031751
50.0000	.080324	.060235	.045170	.033872	.025401	.019048	.014284	.010711	.0080324

TABLE III. - INTEGRAL IN EXPONENT OF PENETRATION PROBABILITY

(a) $0 \leq \delta \leq 1$

α	δ							
	0	0.1	0.2	0.4	0.6	0.8	0.9	1.0
0.0000	1.00000	1.00000	1.00000	1.00000	1.00000	1.00000	1.00000	1.00000
.1000	.98168	.98206	.98243	.98319	.98394	.98469	.98507	.98545
.2000	.93704	.93855	.94007	.94311	.94615	.94919	.95072	.95224
.4000	.78876	.79496	.80117	.81362	.82611	.83865	.84494	.85126
.6000	.57681	.59110	.60545	.63431	.66338	.69266	.70739	.72216
.8000	.31166	.33774	.36399	.41697	.47060	.52488	.55226	-----
.9000	.16132	.19476	.22846	-----	-----	-----	-----	-----
1.0000	.00000	.041847	.084081	.16970	.25682	.34546	.39033	.43561
1.0263	-----	.00000	-----	-----	-----	-----	-----	-----
1.0557	-----	-----	.00000	-----	-----	-----	-----	-----
1.1270	-----	-----	-----	.00000	-----	-----	-----	-----
1.2000	-----	-----	-----	-----	.029275	.16280	.23065	-----
1.2251	-----	-----	-----	-----	.00000	-----	-----	-----
1.3820	-----	-----	-----	-----	-----	.00000	-----	-----
1.4000	-----	-----	-----	-----	-----	-----	.081262	.17954
1.5195	-----	-----	-----	-----	-----	-----	.00000	-----
2.0000	-----	-----	-----	-----	-----	-----	-----	.00000

(b) $1 \leq \delta \leq 5$

α	δ					
	1.0	1.2	1.4	2.0	3.0	5.0
0.00000	1.00000	1.00000	1.00000	1.00000	1.00000	1.00000
.10000	.98545	.98599	.98638	.98721	.98809	.98914
.40000	.85126	.86033	.86699	.88105	.89594	.91379
1.00000	.43561	.49868	.54289	.63051	.71342	.79787
2.00000	.00000	.15455	.25607	.44241	.60023	.74176
4.00000	-----	.081782	.17392	.37586	.55919	.72254
10.00000	-----	.069981	.15588	.35710	.54672	.71668
20.00000	-----	.068509	.15345	.35423	.54491	.71515
50.00000	-----	.065027	.15285	.35630	.54466	.67671

TABLE IV. - PENETRATION PROBABILITY

(a) $\delta = 0$

α	Electrostatic field, E, V/cm								
	10^5	$10^{5.5}$	10^6	$10^{6.5}$	10^7	$10^{7.5}$	10^8	$10^{8.5}$	10^9
0.00000	0	0	0	0	0	0	0	0	0
.10000	-----	-----	-----	-----	-----	$<10^{-37}$	$<10^{-37}$	$<10^{-37}$	$<10^{-37}$
.20000	-----	$<10^{-37}$	$<10^{-37}$	$<10^{-37}$	$<10^{-37}$	0.22877×10^{-30}	0.10539×10^{-22}	0.58820×10^{-17}	0.11994×10^{-12}
.40000	$<10^{-37}$	0.14576×10^{-28}	0.23756×10^{-21}	0.60830×10^{-16}	0.69152×10^{-12}	$.76057 \times 10^{-9}$	$.14515 \times 10^{-6}$	$.74488 \times 10^{-5}$	$.14276 \times 10^{-3}$
.60000	0.49303×10^{-15}	$.33210 \times 10^{-11}$	$.24670 \times 10^{-8}$	$.35078 \times 10^{-6}$	$.14436 \times 10^{-4}$	$.23448 \times 10^{-3}$	$.18966 \times 10^{-2}$	$.90941 \times 10^{-2}$	$.29464 \times 10^{-1}$
.80000	$.42462 \times 10^{-5}$	$.93664 \times 10^{-4}$	$.95303 \times 10^{-3}$	$.54281 \times 10^{-2}$	$.20009 \times 10^{-1}$	$.53223 \times 10^{-1}$.11084	.19215	.29027
.90000	$.46749 \times 10^{-2}$	$.17889 \times 10^{-1}$	$.48935 \times 10^{-1}$.10408	.18328	.28017	.38514	.48894	.58476
1.00000	1.00000	1.00000	1.00000	1.00000	1.00000	1.00000	1.00000	1.00000	1.00000

(b) $\delta = 0.1$

α	Electrostatic field, E, V/cm								
	10^5	$10^{5.5}$	10^6	$10^{6.5}$	10^7	$10^{7.5}$	10^8	$10^{8.5}$	10^9
0.00000	0	0	0	0	0	0	0	0	0
.10000	-----	-----	-----	-----	-----	$<10^{-37}$	$<10^{-37}$	$<10^{-37}$	$<10^{-37}$
.20000	-----	$<10^{-37}$	$<10^{-37}$	$<10^{-37}$	$<10^{-37}$	0.20408×10^{-30}	0.96737×10^{-23}	0.55160×10^{-17}	0.11430×10^{-12}
.40000	$<10^{-37}$	0.86513×10^{-29}	0.16065×10^{-21}	0.45365×10^{-16}	0.55497×10^{-12}	$.64491 \times 10^{-9}$	$.12826 \times 10^{-6}$	$.67889 \times 10^{-5}$	$.13317 \times 10^{-3}$
.60000	0.20588×10^{-15}	$.17254 \times 10^{-11}$	$.15097 \times 10^{-8}$	$.24272 \times 10^{-6}$	$.10953 \times 10^{-4}$	$.19062 \times 10^{-3}$	$.16238 \times 10^{-2}$	$.80945 \times 10^{-2}$	$.27000 \times 10^{-1}$
.80000	$.15084 \times 10^{-5}$	$.43102 \times 10^{-4}$	$.53252 \times 10^{-3}$	$.35083 \times 10^{-2}$	$.14424 \times 10^{-1}$	$.41640 \times 10^{-1}$	$.92210 \times 10^{-1}$.16738	.26173
.90000	$.15372 \times 10^{-2}$	$.77685 \times 10^{-2}$	$.26180 \times 10^{-1}$	$.65110 \times 10^{-1}$.12893	.21521	.31602	.42154	.52321
1.00000	.30471	.41017	.51259	.60584	.68674	.75441	.80951	.85344	.88795
1.02630	1.00000	1.00000	1.00000	1.00000	1.00000	1.00000	1.00000	1.00000	1.00000

(c) $\delta = 0.2$

[illegible]

(d) $\delta = 0.4$

[illegible]

TABLE IV. - Continued. PENETRATION PROBABILITY

(e) $\delta = 0.6$

α	Electrostatic field, E, V/cm								
	10^5	$10^{5.5}$	10^6	$10^{6.5}$	10^7	$10^{7.5}$	10^8	$10^{8.5}$	10^9
0.00000	0	0	0	0	0	0	0	0	0
.10000	-----	-----	-----	-----	-----	$<10^{-37}$	$<10^{-37}$	$<10^{-37}$	$<10^{-37}$
.20000	-----	$<10^{-37}$	$<10^{-37}$	$<10^{-37}$	$<10^{-37}$	0.11518×10^{-30}	0.62997×10^{-23}	0.39989×10^{-17}	0.89805×10^{-13}
.40000	$<10^{-37}$	0.62829×10^{-30}	0.22481×10^{-22}	0.10381×10^{-16}	0.18365×10^{-12}	$.28141 \times 10^{-9}$	$.68868 \times 10^{-7}$	$.42586 \times 10^{-5}$	$.93869 \times 10^{-4}$
.60000	0.24871×10^{-17}	$.62897 \times 10^{-13}$	$.12600 \times 10^{-9}$	$.37698 \times 10^{-7}$	$.27104 \times 10^{-5}$	$.66890 \times 10^{-4}$	$.74039 \times 10^{-3}$	$.44919 \times 10^{-2}$	$.17361 \times 10^{-1}$
.80000	$.77342 \times 10^{-8}$	$.82636 \times 10^{-6}$	$.27449 \times 10^{-4}$	$.37964 \times 10^{-3}$	$.27220 \times 10^{-2}$	$.11925 \times 10^{-1}$	$.36102 \times 10^{-1}$	$.82852 \times 10^{-1}$.15447
1.00000	$.67994 \times 10^{-3}$	$.42139 \times 10^{-2}$	$.16549 \times 10^{-1}$	$.46160 \times 10^{-1}$	$.99618 \times 10^{-1}$.17736	.27335	.37810	.48222
1.20000	.53129	.62234	.70072	.76590	.81873	.86073	.89363	.91912	.93871
1.22510	1.00000	1.00000	1.00000	1.00000	1.00000	1.00000	1.00000	1.00000	1.00000

(f) $\delta = 0.8$

α	Electrostatic field, E, V/cm								
	10^5	$10^{5.5}$	10^6	$10^{6.5}$	10^7	$10^{7.5}$	10^8	$10^{8.5}$	10^9
0.00000	0	0	0	0	0	0	0	0	0
.10000	-----	-----	-----	-----	-----	$<10^{-37}$	$<10^{-37}$	$<10^{-37}$	$<10^{-37}$
.20000	-----	$<10^{-37}$	$<10^{-37}$	$<10^{-37}$	$<10^{-37}$	0.91595×10^{-31}	0.53050×10^{-23}	0.35154×10^{-17}	0.81532×10^{-13}
.40000	$<10^{-37}$	0.21864×10^{-30}	0.10187×10^{-22}	0.57341×10^{-17}	0.11767×10^{-12}	$.20155 \times 10^{-9}$	$.53617 \times 10^{-7}$	$.35298 \times 10^{-5}$	$.81543 \times 10^{-4}$
.60000	0.41546×10^{-18}	$.16438 \times 10^{-13}$	$.46061 \times 10^{-10}$	$.17725 \times 10^{-7}$	$.15391 \times 10^{-5}$	$.43759 \times 10^{-4}$	$.53859 \times 10^{-3}$	$.35383 \times 10^{-2}$	$.14516 \times 10^{-1}$
.80000	$.89715 \times 10^{-9}$	$.16429 \times 10^{-6}$	$.81738 \times 10^{-5}$	$.15306 \times 10^{-3}$	$.13774 \times 10^{-2}$	$.71546 \times 10^{-2}$	$.24613 \times 10^{-1}$	$.62165 \times 10^{-1}$.12453
1.00000	$.54859 \times 10^{-4}$	$.63810 \times 10^{-3}$	$.40179 \times 10^{-2}$	$.15968 \times 10^{-1}$	$.44940 \times 10^{-1}$	$.97638 \times 10^{-1}$.17471	.27028	.37491
1.20000	$.29685 \times 10^{-1}$	$.71543 \times 10^{-1}$.13837	.22692	.32883	.43429	.53503	.62562	.70348
1.38200	1.00000	1.00000	1.00000	1.00000	1.00000	1.00000	1.00000	1.00000	1.00000

TABLE IV. - Continued. PENETRATION PROBABILITY

(gg) $\delta = 0.9$

[illegible]

(h) $\delta = 1$

[illegible]

TABLE IV. - Continued. PENETRATION PROBABILITY

(i) $\delta = 1.2$

α	Electrostatic field, E, V/cm								
	10^5	$10^{5.5}$	10^6	$10^{6.5}$	10^7	$10^{7.5}$	10^8	$10^{8.5}$	10^9
0.00000	0	0	0	0	0	0	0	0	0
.10000	-----	$<10^{-37}$	$<10^{-37}$	$<10^{-37}$	$<10^{-37}$	$<10^{-37}$	$<10^{-37}$	$<10^{-37}$	$<10^{-37}$
.40000	$<10^{-37}$	0.35257×10^{-31}	0.25927×10^{-23}	0.20550×10^{-17}	0.54511×10^{-13}	0.11318×10^{-9}	0.34784×10^{-7}	0.25516×10^{-5}	0.63930×10^{-4}
1.00000	0.70728×10^{-6}	$.24426 \times 10^{-4}$	$.34783 \times 10^{-3}$	$.25491 \times 10^{-2}$	$.11352 \times 10^{-1}$	$.34794 \times 10^{-1}$	$.80591 \times 10^{-1}$.15130	.24264
2.00000	.21188	.31234	.41786	.51977	.61219	.69213	.75885	.81308	.85626
4.00000	.74803	.80436	.84937	.88477	.91228	.93347	.94968	.96203	.97139
10.00000	.93909	.95397	.96528	.97385	.98032	.98521	.98889	.99165	.99374
20.00000	.97848	.98382	.98784	.99087	.99314	.99486	.99614	.99710	.99783
50.00000	.99479	.99609	.99707	.99780	.99835	.99876	.99907	.99930	.99948

(j) $\delta = 1.4$

α	Electrostatic field, E, V/cm								
	10^5	$10^{5.5}$	10^6	$10^{6.5}$	10^7	$10^{7.5}$	10^8	$10^{8.5}$	10^9
0.00000	0	0	0	0	0	0	0	0	0
.10000	-----	$<10^{-37}$	$<10^{-37}$	$<10^{-37}$	$<10^{-37}$	$<10^{-37}$	$<10^{-37}$	$<10^{-37}$	$<10^{-37}$
.40000	$<10^{-37}$	0.20126×10^{-31}	0.17028×10^{-23}	0.14993×10^{-17}	0.43034×10^{-13}	0.94791×10^{-10}	0.30454×10^{-7}	0.23095×10^{-5}	0.59325×10^{-4}
1.00000	0.20152×10^{-6}	$.95269 \times 10^{-5}$	$.17169 \times 10^{-3}$	$.15013 \times 10^{-2}$	$.76320 \times 10^{-2}$	$.25835 \times 10^{-1}$	$.64465 \times 10^{-1}$.12797	.21401
2.00000	$.76452 \times 10^{-1}$.14543	.23555	.33817	.44350	.54351	.63305	.70974	.77328
4.00000	.53934	.62940	.70667	.77078	.82264	.86380	.89602	.92097	.94013
10.00000	.86937	.90034	.92430	.94268	.95670	.96735	.97541	.98151	.98610
20.00000	.95245	.96412	.97297	.97966	.98471	.98851	.99137	.99352	.99514
50.00000	.98780	.99084	.99312	.99484	.99612	.99709	.99782	.99836	.99877

TABLE IV. - Continued. PENETRATION PROBABILITY

(k) $\delta = 2$

α	Electrostatic field, E, V/cm								
	10^5	$10^{5.5}$	10^6	$10^{6.5}$	10^7	$10^{7.5}$	10^8	$10^{8.5}$	10^9
0.00000	0	0	0	0	0	0	0	0	0
.10000	-----	$<10^{-37}$	$<10^{-37}$	$<10^{-37}$	$<10^{-37}$	$<10^{-37}$	$<10^{-37}$	$<10^{-37}$	$<10^{-37}$
.40000	$<10^{-37}$	0.61579×10^{-32}	0.70062×10^{-24}	0.77031×10^{-18}	0.26117×10^{-13}	0.65181×10^{-10}	0.22997×10^{-7}	0.18709×10^{-5}	0.50658×10^{-4}
1.00000	0.16736×10^{-7}	$.14742 \times 10^{-5}$	$.42368 \times 10^{-4}$	$.52570 \times 10^{-3}$	$.34746 \times 10^{-2}$	$.14320 \times 10^{-1}$	$.41414 \times 10^{-1}$	$.91835 \times 10^{-1}$.16687
2.00000	$.11772 \times 10^{-1}$	$.35755 \times 10^{-1}$	$.82254 \times 10^{-1}$.15363	.24544	.34876	.45388	.55302	.64134
4.00000	.26335	.36767	.47222	.56969	.65578	.72877	.78878	.83700	.87509
10.00000	.72564	.78624	.83499	.87351	.90356	.92677	.94457	.95814	.96844
20.00000	.89362	.91912	.93871	.95368	.96506	.97368	.98020	.98511	.98882
50.00000	.97179	.97877	.98403	.98800	.99099	.99324	.99492	.99619	.99714

(l) $\delta = 3$

α	Electrostatic field, E, V/cm								
	10^5	$10^{5.5}$	10^6	$10^{6.5}$	10^7	$10^{7.5}$	10^8	$10^{8.5}$	10^9
0.00000	0	0	0	0	0	0	0	0	0
.10000	-----	$<10^{-37}$	$<10^{-37}$	$<10^{-37}$	$<10^{-37}$	$<10^{-37}$	$<10^{-37}$	$<10^{-37}$	$<10^{-37}$
.40000	$<10^{-37}$	0.17596×10^{-32}	0.27386×10^{-24}	0.38084×10^{-18}	0.15400×10^{-13}	0.43862×10^{-10}	0.17087×10^{-7}	0.14973×10^{-5}	0.42865×10^{-4}
1.00000	0.15886×10^{-8}	$.25216 \times 10^{-6}$	$.11271 \times 10^{-4}$	$.19476 \times 10^{-3}$	$.16501 \times 10^{-2}$	$.81927 \times 10^{-2}$	$.27245 \times 10^{-1}$	$.67086 \times 10^{-1}$.13186
2.00000	$.24137 \times 10^{-2}$	$.10897 \times 10^{-1}$	$.33742 \times 10^{-1}$	$.78757 \times 10^{-1}$.14871	.23952	.34243	.44769	.54735
4.00000	.13738	.22570	.32750	.43297	.53381	.62455	.70258	.76743	.81996
10.00000	.61202	.69199	.75874	.81298	.85619	.89009	.91639	.93662	.95209
20.00000	.84113	.87832	.90729	.92964	.94676	.95980	.96970	.97719	.98285
50.00000	.95719	.96773	.97570	.98172	.98626	.98968	.99225	.99418	.99563

TABLE IV. - Concluded. PENETRATION PROBABILITY

(m) $\delta = 5$

α	Electrostatic field, E, V/cm								
	10^5	$10^{5.5}$	10^6	$10^{6.5}$	10^7	$10^{7.5}$	10^8	$10^{8.5}$	10^9
0.00000	0	0	0	0	0	0	0	0	0
.10000	-----	$<10^{-37}$	$<10^{-37}$	$<10^{-37}$	$<10^{-37}$	$<10^{-37}$	$<10^{-37}$	$<10^{-37}$	$<10^{-37}$
.40000	$<10^{-37}$	0.39145×10^{-33}	0.88725×10^{-25}	0.16356×10^{-18}	0.81705×10^{-14}	0.27270×10^{-10}	0.11964×10^{-7}	0.11462×10^{-5}	0.35080×10^{-4}
1.00000	0.14437×10^{-9}	$.41750 \times 10^{-7}$	$.29260 \times 10^{-5}$	$.70842 \times 10^{-4}$	$.77296 \times 10^{-3}$	$.46392 \times 10^{-2}$	$.11786 \times 10^{-1}$	$.48724 \times 10^{-1}$.10374
2.00000	$.58278 \times 10^{-3}$	$.37538 \times 10^{-2}$	$.15174 \times 10^{-1}$	$.43254 \times 10^{-1}$	$.94877 \times 10^{-1}$.17099	.26596	.37040	.47484
4.00000	$.76925 \times 10^{-1}$.14611	.23637	.33905	.44437	.54431	.63374	.71032	.77376
10.00000	.52539	.61715	.69633	.76230	.81585	.85845	.89185	.91775	.93767
20.00000	.79687	.84343	.88013	.90869	.93071	.94758	.96043	.97017	.97755
50.00000	.94709	.96006	.96990	.97734	.98296	.98719	.99038	.99278	.99458

2/22/85
of

"The aeronautical and space activities of the United States shall be conducted so as to contribute . . . to the expansion of human knowledge of phenomena in the atmosphere and space. The Administration shall provide for the widest practicable and appropriate dissemination of information concerning its activities and the results thereof."

—NATIONAL AERONAUTICS AND SPACE ACT OF 1958

NASA SCIENTIFIC AND TECHNICAL PUBLICATIONS

TECHNICAL REPORTS: Scientific and technical information considered important, complete, and a lasting contribution to existing knowledge.

TECHNICAL NOTES: Information less broad in scope but nevertheless of importance as a contribution to existing knowledge.

TECHNICAL MEMORANDUMS: Information receiving limited distribution because of preliminary data, security classification, or other reasons.

CONTRACTOR REPORTS: Technical information generated in connection with a NASA contract or grant and released under NASA auspices.

TECHNICAL TRANSLATIONS: Information published in a foreign language considered to merit NASA distribution in English.

TECHNICAL REPRINTS: Information derived from NASA activities and initially published in the form of journal articles.

SPECIAL PUBLICATIONS: Information derived from or of value to NASA activities but not necessarily reporting the results of individual NASA-programmed scientific efforts. Publications include conference proceedings, monographs, data compilations, handbooks, sourcebooks, and special bibliographies.

Details on the availability of these publications may be obtained from:

SCIENTIFIC AND TECHNICAL INFORMATION DIVISION
NATIONAL AERONAUTICS AND SPACE ADMINISTRATION
Washington, D.C. 20546